Batrachotoxin-modified Sodium Channels in Planar Lipid Bilayers

Ion Permeation and Block

W. N. GREEN, L. B. WEISS, and O. S. ANDERSEN

From the Department of Physiology and Biophysics, Cornell University Medical College, New York 10021

ABSTRACT Batrachotoxin-modified, voltage-dependent sodium channels from canine forebrain were incorporated into planar lipid bilayers. Single-channel conductances were studied for [Na^+] ranging between 0.02 and 3.5 M. Typically, the single-channel currents exhibited a simple two-state behavior, with transitions between closed and fully open states. Two other conductance states were observed: a subconductance state, usually seen at [NaCl] $\geq$ 0.5 M, and a flickery state, usually seen at [NaCl] $\leq$ 0.5 M. The flickery state became more frequent as [NaCl] was decreased below 0.5 M. The K^+/Na^+ permeability ratio was ~0.16 in 0.5 and 2.5 M salt, independent of the Na^+ mole fraction, which indicates that there are no interactions among permeant ions in the channels. Impermeant and permeant blocking ions (tetraethylammonium, Ca^{++}, Zn^{++}, and K^+) have different effects when added to the extracellular and intracellular solutions, which indicates that the channel is asymmetrical and has at least two cation-binding sites. The conductance vs. [Na^+] relation saturated at high concentrations, but could not be described by a Langmuir isotherm, as the conductance at low [NaCl] is higher than predicted from the data at [NaCl] $\geq$ 1.0 M. At low [NaCl] ($\leq$0.1 M), increasing the ionic strength by additions of impermeant monovalent and divalent cations reduced the conductance, as if the magnitude of negative electrostatic potentials at the channel entrances were reduced. The conductances were comparable for channels in bilayers that carry a net negative charge and bilayers that carry no net charge. Together, these results lead to the conclusion that negative charges on the channel protein near the channel entrances increase the conductance, while lipid surface charges are less important.

INTRODUCTION

Voltage-dependent sodium channels have been characterized in great detail using electrophysiological, biochemical, and, more recently, recombinant DNA techniques. From the electrophysiology of the channels, it has been shown that

Address reprint requests to Dr. Olaf S. Andersen, Dept. of Physiology and Biophysics, Cornell Medical College, 1300 York Ave., New York, NY 10021. Dr. Green's present address is Dept. of Physiology, Yale University School of Medicine, New Haven, CT 06510. Dr. Weiss's present address is Dept. of Anesthesiology, University Medical Center, Tucson, AZ 85724.

J. GEN. PHYSIOL. © The Rockefeller University Press · 0022-1295/87/06/0841/32$1.00

Volume 89 June 1987 841–872

channel function is modulated by maneuvers that appear to alter surface potentials arising from negative charges at the extracellular and intracellular membrane/solution interfaces (Frankenhaeuser and Hodgkin, 1957; Chandler et al., 1965; Drouin and Neumcke, 1974; Hille et al., 1975). Biochemical studies have established that sodium channels carry a net negative charge resulting from an excess of acidic amino acids (Noda et al., 1984, 1986) and from negatively charged carbohydrate chains attached to the protein (Barchi, 1983; J. A. Miller et al., 1983; Messner and Catterall, 1985). The question remains, however, whether the negative charges that appear to modulate function reside on the sodium channel protein or on the surrounding lipid bilayer. In this and the following article (Green et al., 1987), this question is addressed using sodium channels incorporated into planar lipid bilayers of defined composition.

Voltage-dependent sodium channels were incorporated into planar lipid bilayers using the strategy devised by Krueger et al. (1983), where inactivation is removed pharmacologically with the steroidal alkaloid batrachotoxin (BTX) (Daly et al., 1978; Khodorov, 1985). In this article, we describe the permeability characteristics of these BTX-modified channels: the conductance as a function of $[Na^+]$ for sodium channels in neutral and negatively charged phospholipid bilayers, the K^+/Na^+ selectivity, and the inhibition of Na^+ permeation by impermeant monovalent and divalent cations. It is concluded that negative charges on the channel protein are located in the vicinity of the channel entrance, where they serve to increase the local $[Na^+]$. Surface charges on the phospholipid bilayer seem to be less important as modulators of the channel permeability characteristics. Some aspects of this work have been reported previously (Andersen et al., 1986; Green et al., 1986).

MATERIALS AND METHODS

Membrane Formation

Membranes were formed at room temperature (22–25°C), by the pipette method of Szabo et al. (1969), across a hole (~0.3 mm diam) in a Teflon partition separating two Teflon chambers. Each chamber contained 5 ml electrolyte, usually symmetrical NaCl solutions, buffered to pH 7.4 with NaH_2PO_4 (phosphate) or HEPES titrated to pH 7.4 with NaOH. (In the text and figure legends, different solutions are identified by their total cation and buffer concentrations. The major anion in all cases was Cl^-.) The free Ca^{++} concentrations were <1 μM in solutions containing 0.02 and 0.5 M Na^+ (determined using Ca^{++}-selective macroelectrodes made with W. Simon's neutral carrier; we thank Dr. C. O. Lee for assistance with this measurement). The general procedures are described in Andersen and Muller (1982) and Andersen (1983*a*). The membrane-forming solutions were *n*-decane solutions (5% wt/vol) of either a mixture of 1-palmitoyl-2-oleoyl-phosphatidylethanolamine and 1-palmitoyl-2-oleoyl-phosphatidylcholine (molar ratio, 4:1) (PE:PC), or a mixture of 1-palmitoyl-2-oleoyl-phosphatidylethanolamine and 1-palmitoyl-2-oleoyl-phosphatidylserine (molar ratio, 1:1) (PE:PS). Most experiments were done in PE:PC membranes. Experiments in PE:PS membranes are identified in the text. Electrolyte and membrane-forming solutions were made up fresh every 1 or 2 d.

Preparation of Synaptosomes

Dog forebrain synaptosomes were prepared as described by R. S. Cohen et al. (1977). The synaptosomal suspension was collected on a discontinuous sucrose gradient and stored

in 1.0–1.4 M sucrose in small aliquots at −80 to −90°C for up to 4 mo without noticeable loss of activity. The protein concentration of the suspension was 2–6 mg/ml. A freshly thawed sample was used each day. Synaptosomes were usually prepared without protease inhibitors. Some synaptosomes were prepared with the following protease inhibitor mixtures: leupeptin (1.0 μM) and phenylmethylsulfonyl fluoride (PMSF) (0.1 mM); or benzamidine (0.07 mM), PMSF (0.07 mM), trasylol (0.004 mg/ml), and pepstatin A (0.014 mg/ml). No differences were observed between channels from synaptosomes prepared with or without the protease inhibitors.

Electrical Measurements

A standard two-electrode voltage-clamp was used for electrical measurements. Contact with the aqueous solutions was made through Ag/AgCl electrodes. The front electrode was usually in direct contact with the solution. The back electrode was an Ag/AgCl pellet in a microelectrode holder. Contact to the chamber was made through a glass pipette filled with the appropriate electrolyte solution. The same electrode configuration was used for the front electrode in experiments where Cl^- salts were added to the front chamber. The single-channel recordings were generally from channels in the "large" membrane, and the recording bandwidth was <100 Hz owing to the large membrane capacitance (300–400 pF). In some cases, the bilayer punch (Andersen, 1983*a*) was used to isolate sodium channels in smaller membranes (20–80 pF), and the bandwidth could be increased to ~200 Hz. The bilayer punch was also used to remove unwanted channel activity in the membrane. If a "large" membrane showed signs of breakdown or unidentified conductance jumps, the pipette was fused with the bilayer and withdrawn. After this procedure, the membrane frequently regained its original characteristics. Unfortunately, one may also lose the incorporated sodium channels.

The output from the current-to-voltage converter was amplified and filtered with a four- or eight-pole filter with a cutoff frequency between 10 and 100 Hz, usually 20–50 Hz. The output from the filter was displayed on a strip-chart recorder with a frequency response of ~100 Hz.

During experiments, membrane potentials were applied relative to the back chamber. In this article, the following sign convention is used: the aqueous phase facing the tetrodotoxin (TTX)-binding site of the channel is the reference, irrespective of the orientation of the channel(s) in the membrane. The reference solution is denoted the "extracellular" solution. The other solution is denoted the "intracellular" solution. Applied potentials were corrected for electrode asymmetry and liquid junction potentials, which were calculated using the Henderson equation (e.g., Plettig, 1930; Salling and Siggaard-Andersen, 1971).

Channel Incorporation

After the bilayer had thinned, 2–10 μl of an ethanolic stock solution (0.4–0.8 mM) of BTX was added to the back chamber. This addition had no effect on the electrical properties of the membranes (data not shown). A small aliquot (10–50 μl) of the synaptosomal suspension was then added to the front chamber while stirring, and the membrane current (at +60 or −60 mV) was followed as a function of the time to monitor the incorporation of membrane channels, as represented by stepwise increases in the current (see Figs. 1*A* and 3*A*). It was generally not necessary to have an osmotic gradient across the bilayer to achieve channel incorporation (cf. F. S. Cohen, 1986). (In 0.02 M Na^+, channel incorporation seemed to be facilitated by having a salt gradient across the membrane, and incorporations were usually done with 0.1 M Na^+ in the front chamber and 0.02 M Na^+ in the back chamber. After an incorporation, the front chamber was perfused and [Na^+] decreased to 0.02 M.) It was also unnecessary to have Ca^{++} present

when the membranes were formed from PE:PC, but channel incorporation was facilitated by the presence of 0.5–2.0 mM $CaCl_2$ in the front chamber when the membranes were formed from PE:PS. It was usually necessary, however, to break the membrane and form a new bilayer to achieve channel incorporation. This maneuver is probably the reason that some channels incorporated with their TTX-binding site facing the back aqueous phase.

At low [Na^+], channel incorporation was also achieved by mixing the membrane-forming (lipid/decane) solution and the synaptosomal preparation in the Pasteur pipette before blowing the membrane-forming bubble across the hole in the Teflon partition. Channel incorporation usually occurred <5 min after the membrane had thinned down. This procedure resulted in a consistently high yield of channel incorporations. The number of channel incorporations was often high, and a large number of unidentified conductances were observed. It was usually necessary to remove unwanted channel activity with the pipette in the back chamber to obtain membranes that were suitable for further study.

Once a channel was in the membrane, it was identified as a sodium channel if it fulfilled the following criteria: it remained in the open state most of the time in the potential range of −40 to +40 mV; it began to close at membrane potentials between −60 and −100 mV (see above for sign convention for membrane potentials); the channel current was inhibited by TTX (or saxitoxin [STX]); and it had a conductance that was appropriate for the experimental conditions. If the channel could not be identified as a sodium channel, a new membrane was formed. If the channel satisfied the above criteria, any added Ca^{++} was chelated with EDTA, and sometimes the front chamber was perfused to remove the synaptosomes in an attempt to halt further channel incorporation. (Occasionally, channel incorporations were observed later in an experiment, after perfusion of the front chamber. These incorporations may reflect the transfer of new channels into the bilayer from synaptosomes adsorbed to the bilayer [e.g., F. S. Cohen, 1986], or binding of BTX to channels already in the bilayer).

Data Analysis

Single-channel amplitudes were determined from pen-writer records. Single-channel amplitude histograms were assembled from membranes containing one to eight channels. Histograms were collected in absence and presence of extracellular STX or TTX (see Fig. 3, *C* and *D*). It was generally necessary to have guanidinium toxins present to accumulate an acceptable number of single-channel current transitions. (There was no detectable difference in the single-channel amplitudes estimated on the basis of the major peak in histograms based on spontaneous or guanidinium toxin–induced current transitions.) Single-channel conductances were estimated from linear regression analysis of the single-channel current-voltage relations. The conductances were normalized to a temperature of 24°C using a Q_{10} value of 1.3 (Nagy et al., 1983).

Eqs. 1 and 2 (see Results) were fitted to the data using a nonlinear least-squares routine based on a combination of the grid search and Marquardt-Levenberg algorithms (e.g., Bevington, 1969, pp. 204–246). Eqs. 3–5 were fitted to the conductance vs. concentration data using a combination of an interactive fit and a grid search. The quality of the fit was judged visually and by the chi square (χ^2) (e.g., Bevington, 1969, pp. 187–203). Fits of different models to the same data were compared using the F test as suggested by Ellis and Duggleby (1978): $F = (R_1 - R_2)\cdot(n - p_1)/[R_1\cdot(p_1 - p_2)]$, where R_1 and p_1 are the sum of the squared residuals and the number of parameters associated with the more complex model, R_2 and p_2 denote the corresponding parameters for the simpler model, and n is the number of data points. The degrees of freedom for F are $(p_1 - p_2)$ and $(n - p_1)$.

Materials

The lipids were from Avanti Polar Lipids, Inc., Birmingham, AL, and were used without further purification. *n*-Decane was 99.9% pure from Wiley Organics, Columbus, OH; it was sometimes purified over alumina before use. TTX was obtained from Sigma Chemical Co., St. Louis, MO, and STX was obtained from the Food and Drug Administration, Cincinnati, OH. BTX was a generous gift from Dr. John Daly, National Institutes of Health, Bethesda, MD. The inorganic salts were reagent grade. The alkali metal chlorides were roasted for at least 24 h at 500–600°C and stored in evacuated dessicators over NaOH. Tetraethylammonium chloride (TEA-Cl) was recrystallized as described previously (Andersen, 1983*a*). The water was deionized Milli-Q water (Millipore Corp., Bedford, MA).

RESULTS

Sodium Channel Incorporation

After addition of BTX and synaptosomes, the time before channel incorporation varied from <1 to 151 min. This waiting time was usually <30 min. Generally, channel incorporations appeared as rectangular increments in the membrane current. The amplitudes of the current jumps corresponded to multiples of the unitary conductance of the sodium channel. In the absence of BTX, sodium channel incorporations were not observed. (In one experiment, the membrane was monitored for >6 h after the synaptosome addition, but before the addition of BTX. No sodium channel activity was observed, although there was other uncharacterized channel activity. The subsequent addition of BTX led to the appearance of four sodium channels over a 15-min period.)

The statistics on channel incorporation are summarized in Table I. Of 350 incorporation events, there were 5 in which more than four channels incorporated simultaneously. The average number of channels per event was 1.5, with no apparent $[Na^+]$ dependence ($0.02\ M \leq [Na^+] \leq 3.5\ M$). If channel incorporation results from the fusion of a vesicle with the bilayer (C. Miller and Racker, 1976), the distribution of the number of channels per incorporation event should be described by the Poisson distribution. The data in Table I can be described by a Poisson distribution with a mean of 0.5 channels per fusion event. The Poisson mean value is smaller than the observed average because a large number of fusion events (~60%) presumably did not result in channel incorporations.

If the bilayer was not broken in the interval between synaptosome addition and channel incorporation ($n = 15$), the guanidinium toxin–binding site of the incorporated channels faced the compartment where the synaptosomes were added. This orientation of the channels in the bilayer is consistent with outside-out vesicles fusing with the bilayer.

In some cell membranes, sodium channels are immobile (Stühmer and Almers, 1982) and cluster (Almers et al., 1983; Beam et al., 1985). In contrast, sodium channels do not remain in close contact after incorporation into planar bilayers. Channel separation was demonstrated using the bilayer punch to isolate "small" membranes after a single incorporation event of two or more channels. In five instances, one or more channels were isolated in the "small" membrane after a single, multichannel incorporation event. When the pipette was removed from

TABLE I

Number of Channels per Incorporation Event

[Na^+]	Total	1	2	3	4	5	6	>6
M								
0.02	13	10	2	—	1	—	—	—
0.05	29	17	9	2	1	—	—	—
0.1	161	120	29	6	3	—	1	2 (7, 10)
0.2	13	6	2	3	1	—	—	1 (7)
0.5	74	48	17	6	3	—	—	—
1.0	38	25	4	5	4	—	—	—
2.5	15	10	2	1	1	—	1	—
3.5	7	6	1	—	—	—	—	—
Total	350	242	66	23	14	—	2	3

The distribution of the number of channels per incorporation event (x) is described by the Poisson distribution, $N(x) = N \cdot (\lambda^x/x!) \cdot \exp(-\lambda)$, where $N(x)$ is the number of fusion events with x channels, N is the total number of events, and λ is the average number of channels per event. λ can be estimated from the ratio of successive values of $N(x)$: $\lambda = (x + 1) \cdot N(x + 1)/N(x) \cdot \lambda \simeq 0.5$ [from $N(2)/N(1)$], $N = 770$, $N(1) = 240$, $N(2) = 70$, $N(3) = 10$, $N(4) = 2$.

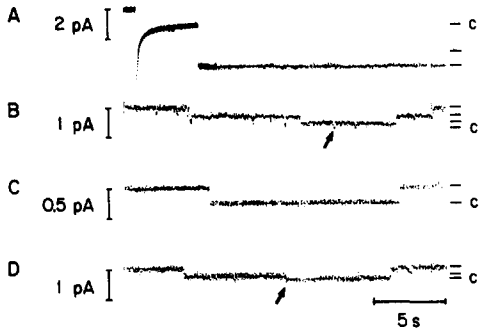

FIGURE 1. The isolation of a single sodium channel after a multichannel incorporation. (*A*) Simultaneous incorporation of three sodium channels. The capacitative transient on the left marks a voltage change from 0 to −60 mV. The incorporation event is visualized as a discrete increase in the membrane current (downward deflection). The amplitude of this initial current transition is approximately three times as large as the amplitude of the single-channel current transitions shown in the trace (at the far right). Experiment 840410: 0.1 M Na^+ plus 0.1 M TEA^+ in the extracellular solution, 0.2 M Na^+ in the intracellular solution, 0.01 M HEPES. (*B*) Current transitions at 0 mV after addition of TTX. Channel openings are upward current transitions. There are transitions between three current levels; two of the three channels undergo long-lived (TTX-induced) transitions. Smaller, short-lived transitions (marked by the arrow) are seen for the third channel. (*C*) Current transitions at 0 mV with a single sodium channel in the pipette. (*D*) Current transitions at 0 mV after the pipette was pulled back from the large membrane. Two channels remained; they display long-lived (TTX-induced) transitions. Current transitions for one channel (marked by the arrow) have the same small amplitude as the transition indicated by an arrow in *B*. (See Figs. 3 and 4 for other examples of such current transitions.)

the bilayer, some or all of the other channels remained in the large membrane. Current traces illustrating the isolation of a single channel after a three-channel incorporation are shown in Fig. 1.

BTX-modified Sodium Channels Disappear Spontaneously

An experiment terminates when there is no longer any observable channel activity. Termination may occur for several reasons: the membrane breaks; channels are removed using the pipette; the membrane changes from a bilayer

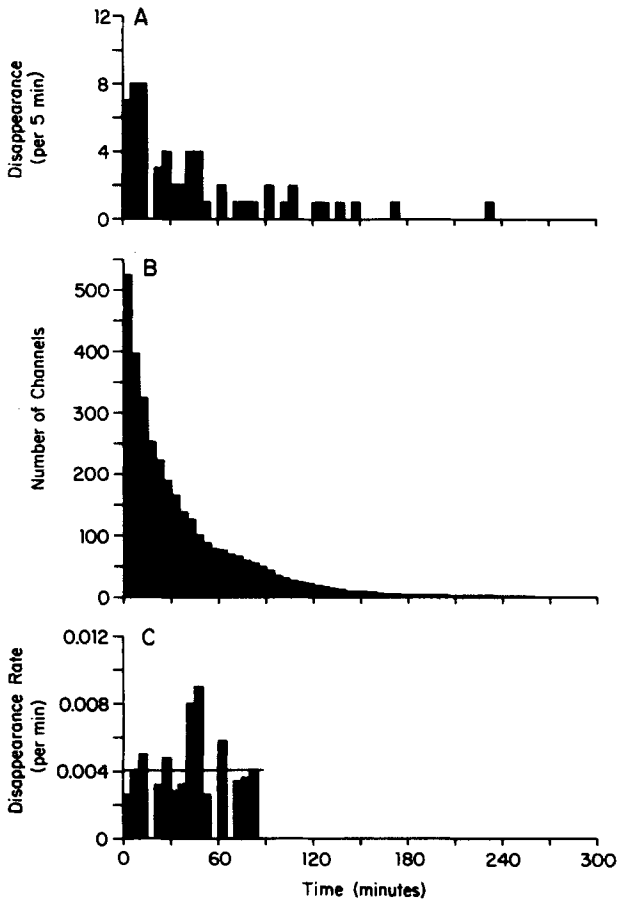

FIGURE 2. The rate of spontaneous sodium channel disappearance. (*A*) Duration histogram of the lifetimes of 59 sodium channels that disappear spontaneously. The lifetimes were accumulated in 5-min bins. (*B*) Survivor plot of the lifetimes of all 524 sodium channels. The lifetimes were accumulated in 5-min bins. (*C*) The spontaneous sodium channel disappearance rate as estimated by dividing the number of events per bin in *A* by the total number of lifetimes in the corresponding bin in *B*. The solid horizontal line at 0.004/min marks the average channel disappearance rate over the first 90 min.

to a thick membrane, as evidenced by a decrease in membrane capacitance; or, for unknown reasons, the channels spontaneously disappear some time after incorporation. These channels were usually normal up to the point of disappearing. One possible cause for channel disappearances is the dissociation of BTX from the channels, in which case the disappearance rate is an upper estimate for the BTX dissociation rate constant.

To obtain an estimate for the spontaneous disappearance rate, the following procedure was used. The distribution of channel lifetimes, the interval from channel appearance to disappearance, for the 59 spontaneously disappearing channels was accumulated into a duration histogram (Fig. 2*A*). In addition, all 524 channel lifetimes were accumulated into a survivor histogram (Fig. 2*B*). For

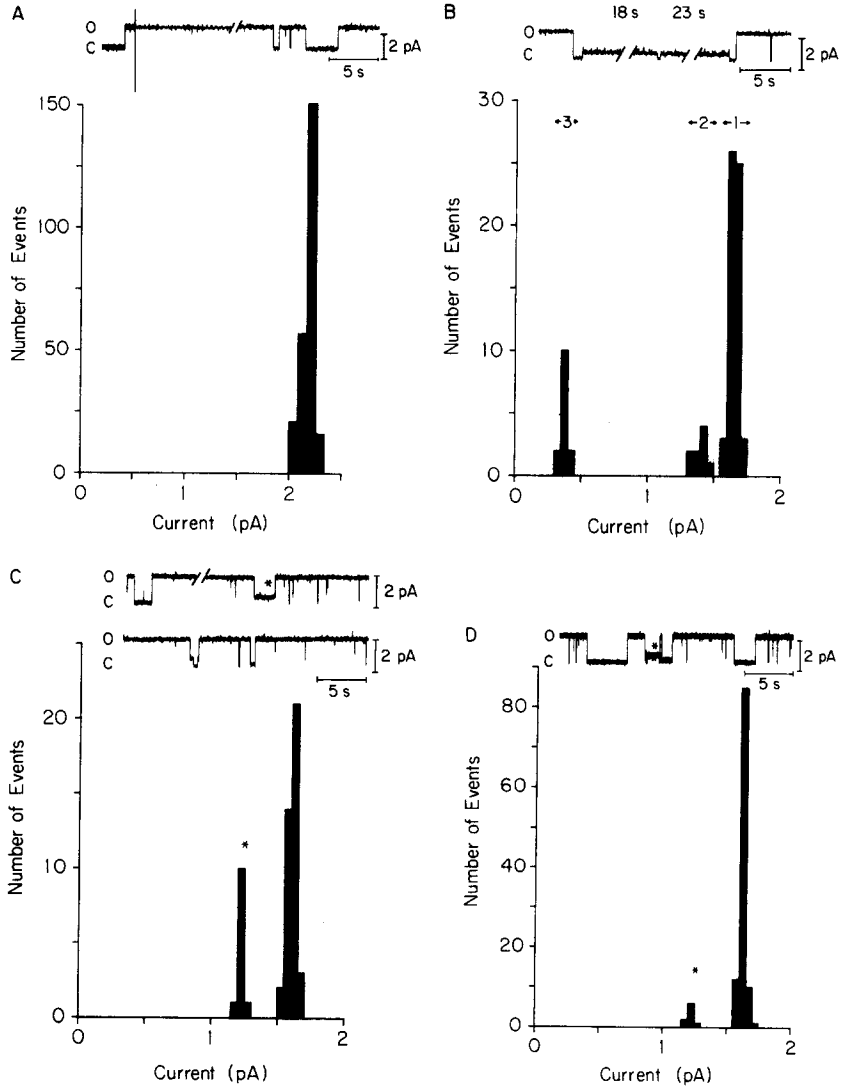

both histograms, the abscissa is the channel lifetime in 5-min bins. The ordinate in Fig. 2*A* denotes the number of spontaneous disappearances that occur within each 5-min interval, while the ordinate in Fig. 2*B* represents the number of remaining channels that have a duration equal to or longer than indicated. The spontaneous channel disappearance rate cannot be determined solely from the histogram in *A* because of the time-dependent decrease in the number of channels in the parent population (*B*). The rate was estimated by dividing the content of each bin in *A* by the content of the corresponding bin in *B*, as displayed in Fig. 2*C*. Over the first 90 min, a time that encompasses >91% of the lifetimes, the rate is quite constant, 0.02 channel disappearances per 5 min, or 0.004 min^{-1}. (The same estimate was obtained by extending the analysis to 120 min, a time that encompasses >96% of all channel lifetimes. The counting error between 90 and 120 min led, however, to large bin-to-bin variations in the estimate of the rate constant.)

Single-Channel Current Amplitudes

Single-channel current traces predominantly exhibit transitions between two states: a "fully open" state, and a closed state as illustrated in the amplitude histograms in Figs. 3*A* and 4*A*. Transitions to partially open or subconductance states and to "flickery" states were also observed. These states fell into two

FIGURE 3. (*opposite*) Single-channel current transitions at high [Na^+]. (*A*) Current trace and amplitude histogram in 2.5 M Na^+. The trace illustrates a single-channel incorporation event as an upward current transition (at the far left). TTX was added during the break in the record, giving rise to long-lived channel closures that were used in compiling the histogram. The average single-channel current, $\bar{i}$, was 2.14 ± 0.06 pA (n = 245), mean ± SD (number of observations). Experiment 831122: 0.01 M phosphate, ΔV = 56 mV, 24°C. (*B*) Current trace and histogram of current transition amplitudes in 1.0 M Na^+. The trace illustrates an example of the substate observed at high [Na^+]. The three peaks in the histogram represent the three different classes of current transitions: (*1*) between the fully closed and the fully open state, with $\bar{i}$ = 1.62 ± 0.03 pA (n = 57); (*2*) between the fully open and the subconductance state, with $\bar{i}$ = 1.4 ± 0.1 pA (n = 9); and (*3*) between the subconductance and the fully closed state, with $\bar{i}$ = 0.35 ± 0.03 pA (n = 14). Experiment 831207: 0.01 M phosphate, ΔV = 62 mV, 21.5°C. (*C*) Current traces and histogram of current transition amplitudes in 0.5 M Na^+ before the addition of TTX. The traces illustrate current transitions to the fully closed state and to the substate (marked by an asterisk). The histogram was compiled from a 13.5-min-long record; the asterisk denotes the peak corresponding to transitions between the fully open and the subconductance state. For transitions between the fully open and closed states, $\bar{i}$ = 1.58 ± 0.04 pA (n = 40); for the transitions between the fully open and the subconductance state, $\bar{i}$ = 1.2 ± 0.1 pA (n = 12). Experiment 850415: 0.01 M HEPES, ΔV = 63 mV, 25°C. (*D*) Current trace and histogram of current transition amplitudes obtained for the same channel as in *C* after the addition of 93 nM TTX. The amplitude histogram was again compiled over 13.5 min. The asterisks in the trace and histogram denote subconductance states. For transitions between the fully open and closed states, $\bar{i}$ = 1.60 ± 0.02 pA (n = 108); for transitions between the fully open and the subconductance state, $\bar{i}$ = 1.2 ± 0.1 pA (n = 9).

categories, a "high-salt" subconductance type (Fig. 3), and a "low-salt" flickery type (Fig. 4).

The subconductance state was observed mostly at $[Na^+] \geq 0.5$ M. The subconductance current amplitude was typically 0.2–0.3 of the "fully open" amplitude, with little increase in the peak-to-peak current noise (Fig. 3*B*). The subconductance state does not represent an aberrant form of the channel closures induced

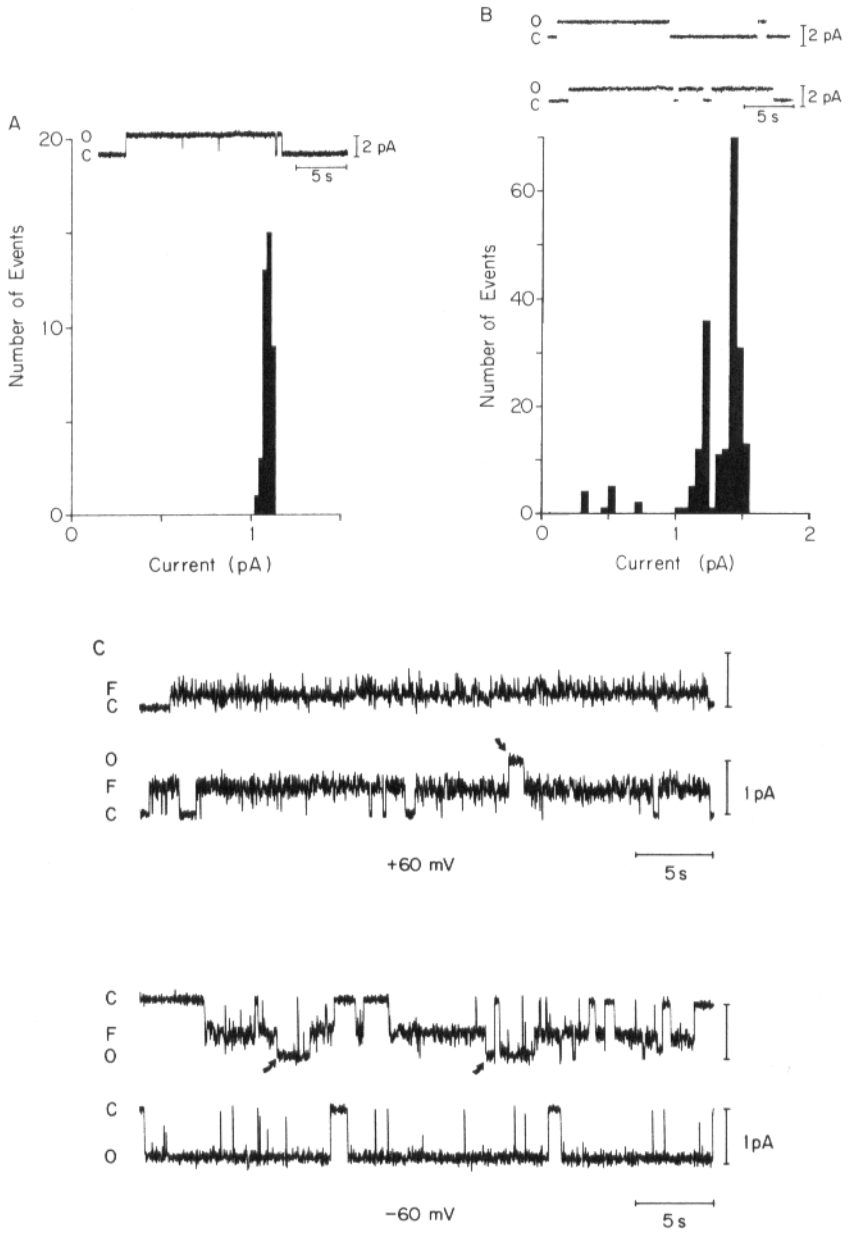

by STX and TTX, which increase the number and duration of transitions from the open to the closed state. This toxin independence is illustrated in Fig. 3, *C* and *D*, where the amplitude histograms were compiled over roughly the same amount of time, before and after the addition of TTX. The peak representing transitions between the fully open and the closed states increased after toxin addition, while the peak for transitions to the subconductance state decreased because the total time the channel was in the open state decreased. In addition, toxin-induced closures from the subconductance state were observed.

The flickery state was observed mostly at $[Na^+] \leq 0.5$ M. It is characterized by an increase in the peak-to-peak noise of the open-state current. Examples are shown in Fig. 4, *B* and *C* (see also Andersen et al., 1986). The increase in the current noise indicates that channels in this state fluctuate between two or more conductance states. The peaks in the amplitude histograms that correspond to transitions to the flickery state represent estimates of the time-averaged current amplitude, and cannot readily be used to characterize Na^+ permeation through the channel. Unlike the subconductance state observed at high $[Na^+]$, the time-averaged current of the flickery state varied from channel to channel and even with time and membrane potential for a given channel (Fig. 4*C*). The flickery state cannot result from shifts in the voltage activation of the channels (e.g., Weiss et al., 1984). This is most clearly seen by comparing the traces obtained at −60 and +60 mV in Fig. 4*C*, where the flickery state is most pronounced at positive potentials.

The flickery state became more frequent as the $[Na^+]$ was lowered. In 0.02 M Na^+, more than half the channels exhibited this type of behavior. In some instances, only a flickery state was observed. Additionally, the time-averaged current in the flickery state seemed to decrease relative to the "fully open state" current as the $[Na^+]$ was lowered. In 0.02 M Na^+, the time-averaged current could be less than half the "fully open state" current (see Fig. 4*C*). The existence of the flickery state necessitated careful inspection of the current records to

---

FIGURE 4. (*opposite*) Single-channel current transitions at low $[Na^+]$. (*A*) Current trace and amplitude histogram in 0.02 M Na^+. The trace illustrates current transitions for a channel that predominantly undergoes transitions between the fully open and the fully closed states. $\bar{i} = 1.10 \pm 0.02$ pA ($n = 41$). Experiment 860122: 0.01 HEPES, $\Delta V = 60$ mV. (*B*) Current trace and histogram of current transition amplitudes in 0.1 M Na^+. The traces illustrate transitions between the fully open and the closed state (top trace) and between the flickery and the closed state (bottom trace). There is an increased peak-to-peak current noise of the open channel in the bottom trace. In the histogram, the peak to the right corresponds to transitions between the fully open and closed states, with $\bar{i} = 1.41 \pm 0.05$ pA ($n = 138$). The peak immediately to the left corresponds to transitions between the flickery and the closed states, with $\bar{i} = 1.18 \pm 0.04$ pA ($n = 56$). Experiment 830907: 0.01 M phosphate, $\Delta V = 60$ mV. (*C*) Current traces illustrating the behavior of a flickery state for a single channel in 0.02 M Na^+. The open current changes with membrane potential and time. At both +60 and −60 mV, the top traces were recorded ~15 min before the bottom traces. The arrows indicate transitions to what appears to be the fully open state. Experiment 860121: 0.005 M phosphate, 22.5°C.

ensure that only current transitions to the fully open state were included in histograms used to determine the single-channel conductance. The rest of the Results section will describe the behavior of the fully open state of the sodium channel.

Single-Channel Conductance

At each [Na^+], the single-channel current-voltage (*i-V*) relations were determined from the mean currents obtained from amplitude histograms at different mem-

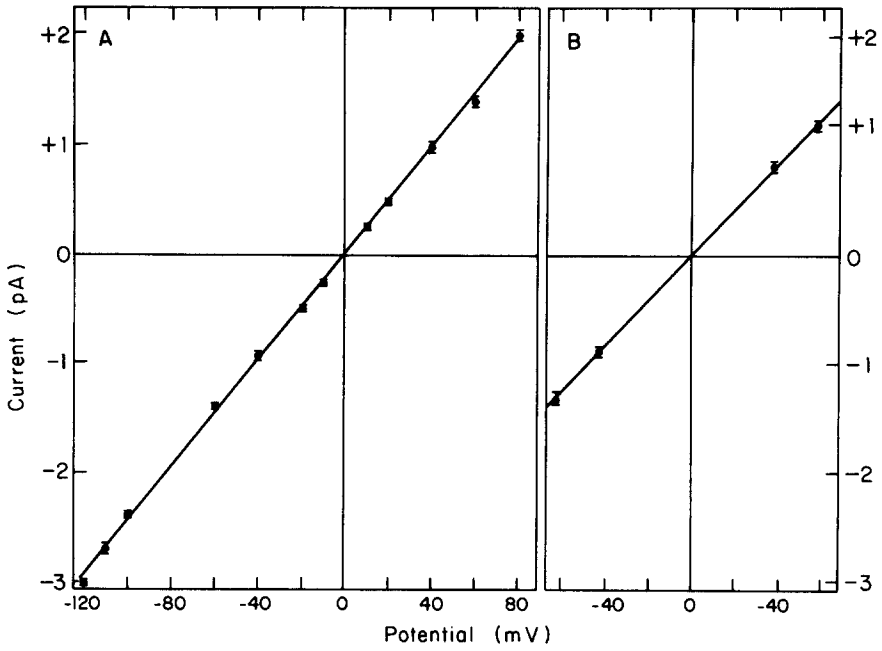

FIGURE 5. Current-voltage relations in symmetrical solutions. (*A*) *i-V* relation for a channel in a membrane carrying no net charge. The symbols denote means ± SD. The line denotes a linear regression to the data. The conductance was 24.7 pS (r = 0.9997). Experiment 830907: 0.1 M Na^+, 0.01 M phosphate, PE:PC (4:1). (*B*) *i-V* relation for a channel in a membrane carrying a negative net charge. The line denotes a linear regression to the data. The conductance was 21.0 pS (r = 0.9999). Experiment 830830: 0.1 M Na^+, 0.01 M phosphate, PE:PS (1:1).

brane potentials. In symmetrical NaCl, the *i-V* relations were linear for [Na^+] ranging between 0.02 and 3.5 M (e.g., Fig. 5) and the conductances were determined from the slopes of the *i-V* relations.

The single-channel conductance, g, varies as a function of [Na^+] (Fig. 6). The g-[Na^+] relation tends toward a limiting value at high [Na^+] (Fig. 6*A*), but cannot be described by a simple rectangular hyperbola, as shown by the nonlinear Eadie-Hofstee plot of the data (Fig. 6*B*). The nonlinearity of the Eadie-Hofstee plot appears to result from a net negative charge in the vicinity of the channel entrance(s), which gives rise to an electrostatic potential difference between the bulk solution and the entrances. This negative potential difference will increase

the local [Na^+] and thus the single-channel conductance (Drouin and Neumcke, 1974). The solid curves in Fig. 6, *A* and *B*, were calculated based on a model assuming a net negative charge at the channel entrance (see the Discussion).

When channels were incorporated into bilayers formed from PE:PS, which should carry a net negative surface charge, the single-channel conductances at [Na^+] = 0.1 or 0.5 M were 21.6 and 25.5 pS, which compares well with the corresponding conductances measured in PE:PC membranes: 21.7 and 25.3 pS.

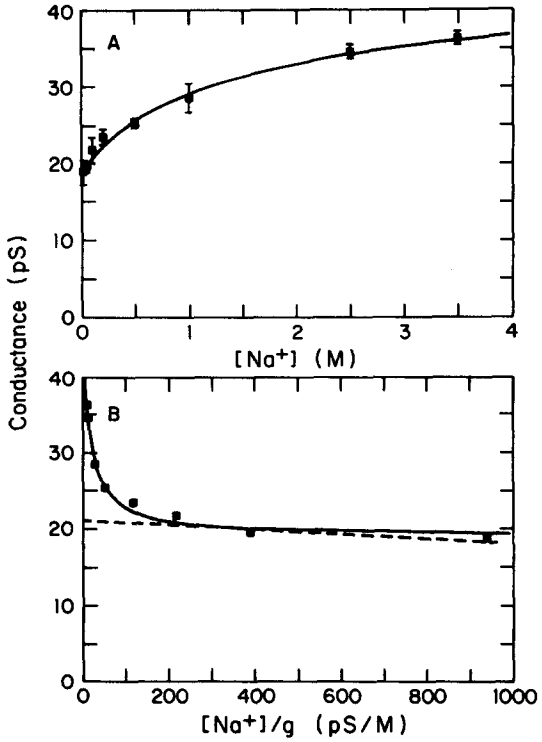

FIGURE 6. Conductance vs. [Na^+]. (*A*) g-[Na^+] relation for channels in net neutral PE:PC membranes. The points denote means ± S.D. The curve denotes a fit of Eqs. 3–5 to the data (see Discussion): g_{max} = 45 pS, K_{Na} = 1.5 M, σ = −0.38 $e \cdot nm^{-2}$, χ^2 = 2.6. (*B*) Eadie-Hofstee plot of the data in *A*. The solid line denotes a transform of the solid curve in *A*; the dotted line denotes a nonlinear least-squares fit of Eq. 5 to the data for 0.02 M ≤ [Na^+] ≤ 0.1 M (assuming σ = 0), g_{max} = 21 pS, K_{Na} = 0.003 M, χ^2 = 1.2.

The *i-V* relations were also unaffected (Fig. 5*B*). At these values of [Na^+], negative charges on the lipids have no measurable effect on the [Na^+] at the channel entrance.

Ion Selectivity

Within the error of our measurements, the channels are ideally cation selective. The selectivity was evaluated from the reversal potential, V_{rev}, determined from single-channel *i-V* relations with different ionic compositions in the aqueous

phases. In the presence of an [Na^+] difference (either 0.1 vs. 0.02 M or 0.1 vs. 0.2 M), V_{rev} was within 1 mV of the Na^+ equilibrium potential (Fig. 7). When the ionic strength was not held constant (0.1 vs. 0.02 M), the slope conductance at V_{rev}, 19.6 pS, was between the conductance values found in symmetrical 0.02 M Na^+ (18.8 ± 1.6 pS [± SD]) and 0.1 M Na^+ (21.7 ± 1.7 pS). At constant ionic strength (0.1 vs. 0.2 M), maintained by the addition of tetraethylammonium (TEA^+), the slope conductance at V_{rev}, 19.5 pS, was smaller than the conductance in symmetrical 0.1 M Na^+ (21.7 ± 1.7 pS) or 0.2 M Na^+ (23.4 ± 1.0 pS).

The K^+/Na^+ selectivity was determined from V_{rev}, measured under a variety of ionic conditions, and quantified as the permeability ratio, P_K/P_{Na}, using the

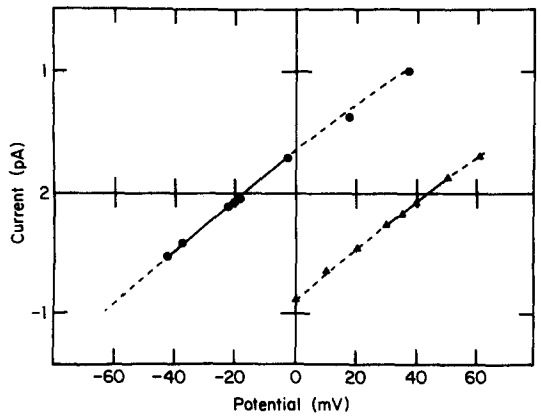

FIGURE 7. *i-V* relations in asymmetric solutions. (▲) 0.1 M in the extracellular and 0.02 M Na^+ in the intracellular solution. V_{rev} was estimated to be 44.0 mV from a linear regression analysis of the currents between 30 and 50 mV (solid region of the line through the points). The Na^+ equilibrium potential (E_{Na}) was 43.0 mV (24°C). The slope conductance at V_{rev} was 19.6 pS. Experiment 840401: 0.005 M phosphate. (●) 0.1 M Na^+ plus 0.1 M TEA^+ in the extracellular solution and 0.2 M Na^+ in the intracellular solution. V_{rev} was estimated to be −16.8 mV from a linear regression fit to the data between −42 and −2 mV (solid region of the line through the points); E_{Na} was −17.7 mV (23.5°C). The slope conductance at V_{rev} was 19.5 pS. Experiment 840410: 0.01 M HEPES.

Goldman-Hodgkin-Katz equation (see Table II). P_K/P_{Na} varied between 0.14 and 0.18. The variation in P_K/P_{Na} reflects variations in V_{rev} of <1 mV, which is smaller than the error in measuring V_{rev}. Under the ionic conditions tested, the channels' selectivity is independent of the concentration and mole fraction of the permeant ions. When the extracellular and intracellular solutions were reversed, P_K/P_{Na} was not affected, but the shape of the *i-V* relation changed (see Fig. 8). The slope conductance at V_{rev} was smaller with K^+ in the intracellular solution, which indicates that intracellular K^+ blocks Na^+ movement through the channel.

Screening and Block by Monovalent and Divalent Cations

Voltage-dependent sodium channels carry a net negative charge (Barchi, 1983; J. A. Miller et al., 1983; Noda et al., 1984, 1986; Messner and Catterall, 1985).

TABLE II

Ion Selectivity of BTX-modified Na Channels

Ionic conditions (extracellular/intracellular)	V_{rev}	P_K/P_{Na}*
M	*mV*	
0.50 Na^+/0.05 Na^+ + 0.45 K^+ (n = 1)	+34.0	0.18
0.50 Na^+/0.25 Na^+ + 0.25 K^+ (n = 2)	+13.8	0.18
0.25 Na^+ + 0.25 K^+/0.50 Na^+ (n = 2)	−13.6	0.16
2.5 Na^+/0.25 Na^+ + 2.25 K^+ (n = 2)	+34.5	0.18
1.25 Na^+ + 1.25 K^+/2.5 Na^+ (n = 1)	−14.5	0.14

* The selectivity is quantified by the permeability ratio, P_K/P_{Na}, which was calculated from the Goldman-Hodgkin-Katz equation (Hodgkin and Katz, 1949): $V_{rev} = -(kT/e)\cdot\ln\{([Na^+]_i + P_K/P_{Na}\cdot[K^+]_i)/([Na^+]_o + P_K/P_{Na}\cdot[K^+]_o)\}$, where the subscripts i and o refer to the extracellular and intracellular solutions, k is Boltzmann's constant, T is the temperature, and e is the elementary charge.

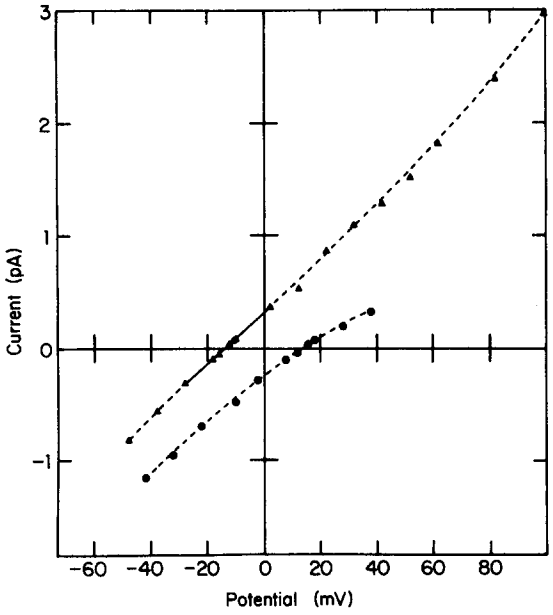

FIGURE 8. Ion selectivity of the channel. (▲) i-V relation with 0.25 M K^+ plus 0.25 M Na^+ in the extracellular solution and 0.5 M Na^+ in the extracellular solution. V_{rev} was estimated to be −13.6 mV from a linear regression to the data between −30 and 2 mV (solid region of the line through the points); P_K/P_{Na} = 0.16. The slope conductance at V_{rev} was 23 pS. Experiment 851113a: 0.01 M HEPES, 24°C. (●) i-V relation with 0.5 M Na^+ in the extracellular solution and 0.25 M K^+ plus 0.25 M Na^+ in the intracellular solution. V_{rev} was estimated to be 14.0 mV from a linear regression to the data between 8 and 18 mV (solid region of the line through the points); P_K/P_{Na} = 0.16. The slope conductance at V_{rev} was 17 pS. Experiment 851113b: 0.01 M HEPES, 24°C.

The shape of the g-[Na^+] relation (Fig. 6*A*) suggests that some of these charges impart a net negative charge to the channel entrances. The experiments described below were in part designed to test whether the single-channel conductance is modulated by a net negative charge at the entrances.

Experiments with TEA$^+$. The effects of TEA^+ on the single-channel current depended on whether TEA^+ was added to the extracellular or intracellular solution. When added to the intracellular solution, the predominant action of TEA^+ was to induce a voltage-dependent block (Fig. 9) similar to that caused by other monovalent or divalent organic cations, e.g., local anesthetics (Strichartz, 1973), quaternary alkylammoniums (Rojas and Rudy, 1976), *N*-alkylguanidiniums (Kirsch et al., 1980), and divalent *N*-alkylguanidium analogues (Danko et al., 1986). Concurrent with the TEA^+-induced block, the peak-to-peak single-channel current noise increased as the membrane potential was increased (Fig. 9*A*). The voltage dependence of the block was described using the relation (Woodhull, 1973):

$$i_B/(i_0 - i_B) = \{K_B(0)/[B]\} \cdot \exp(-z \cdot \delta \cdot \Delta V \cdot e/kT), \quad (1)$$

where i_B is the current in the presence of the blocker, e.g., TEA^+, i_0 is the current in the absence of blocker, $K_B(0)$ is the dissociation constant for the blocker at 0 mV, [B] is the concentration of the blocking ion, z is its valence, δ is the fraction of the membrane potential that is affecting block, ΔV is the membrane potential difference, e is the elementary charge, k is Boltzmann's constant, and T is the temperature in Kelvin. In symmetrical 0.05 M Na^+, the estimates for δ and $K_B(0)$ were -0.54 ± 0.04 and 0.031 ± 0.002 M, respectively (Fig. 9*C*). The negative δ value arises because TEA^+ enters and blocks from the intracellular solution.

When the [TEA^+] was increased, the time-averaged single-channel current amplitude decreased and peak-to-peak noise increased (Fig. 10*A*). The dose-response curves for the intracellular TEA^+-induced block appear to be single-site binding isotherms (Fig. 10*B*), and the voltage dependence of the [TEA^+] for half-maximal block was similar to the voltage dependence of current block at a constant [TEA^+] (squares, Fig. 9*B*).

When added to the extracellular solution, TEA^+ produced a smaller, virtually voltage-independent current reduction (Fig. 7), with no concomitant increase in the open-channel current noise. The current reduction is probably a result of screening of negative charges in the vicinity of the channel entrance, which would reduce the local [Na^+] and thus the current. The screening effect of TEA^+ was evaluated in experiments at a constant ionic strength (0.1 M) at −80 mV, where the net Na^+ flux is almost equal to the unidirectional flux (e.g., Andersen et al., 1986). In symmetrical 0.05 M Na^+ plus 0.05 M TEA^+ solutions, the chord conductance at −80 mV was 13.5 pS, or ~70% of the current in the absence of TEA^+. In symmetrical 0.02 M Na^+ plus 0.08 M TEA^+, the chord conductance at −80 mV was 8.2 pS, or ~40% of the current in the absence of TEA^+.

Effect of divalent cations. In symmetrical solutions of 0.02 M Na^+ plus 0.005 M Ba^{++}, the *i-V* relation was linear, but the conductance was reduced to ~5.4 pS (Fig. 11). The linear *i-V* relation indicates that the effect of Ba^{++} is essentially

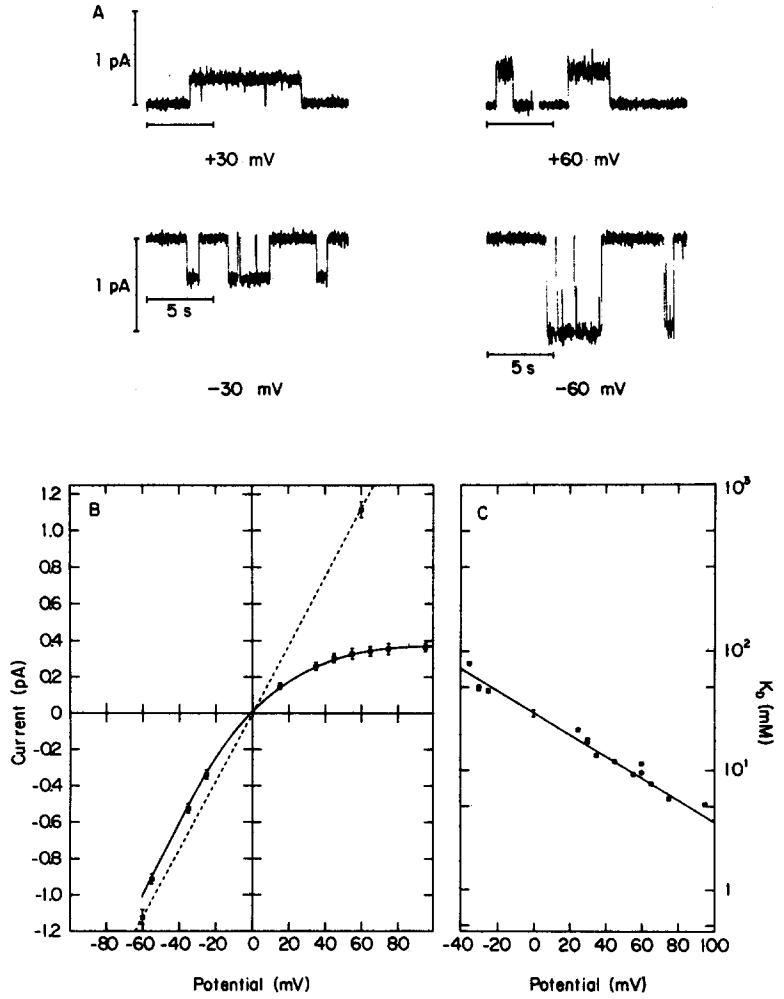

FIGURE 9. Effects of intracellular TEA^+ on single-channel currents. (*A*) Single-channel current traces in the presence of TEA^+. At positive potentials, channel openings are upward; at negative potentials, channel openings are downward. Relative to transitions at negative potentials, the current amplitude decreased, and the open-channel current noise increased at positive potentials. Experiment 851106: 0.05 M Na^+ in the extracellular and 0.05 M Na^+ plus 0.02 M TEA^+ in the intracellular solution, 0.01 M phosphate. (*B*) *i-V* relation in the presence of intracellular TEA^+. The solid curve was drawn by eye. The dashed line represents the average single-channel *i-V* relation in 0.05 M Na^+ in the absence of TEA^+. Experiment 840112: 0.05 M Na^+ in the extracellular solution and 0.05 M Na^+ plus 0.02 M TEA^+ in the intracellular solution, 0.005 M phosphate. (*C*) Voltage dependence of the intracellular TEA^+ block. (■) The data from *B* are plotted as $i_B/(i_0 - i_B)$ vs. ΔV. The line denotes a fit of Eq. 1 to the data: K_B (0) = 3.0 ± 0.2 10^{-2} M, and δ = −0.54 ± 0.04. (●) K_B estimates from the dose-response data of Fig. 10; they were not included in the analysis.

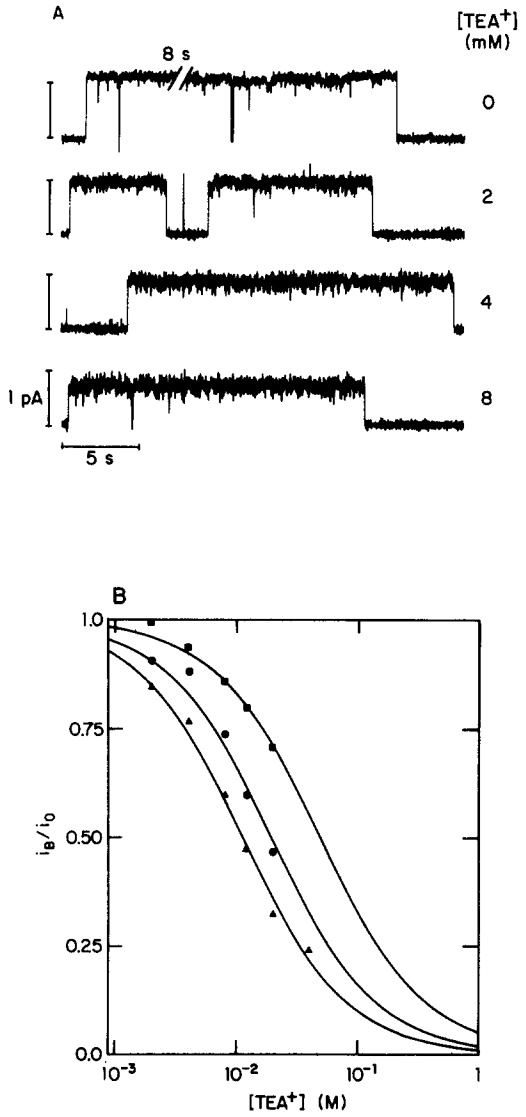

FIGURE 10. Dose-response curves for intracellular TEA^+ block. (*A*) Single-channel current traces at +60 mV in symmetrical 0.05 M Na^+ with or without TEA^+ in intracellular solution. Channel openings are upward. The current amplitude decreased and the channel current noise increased as [TEA^+] increased. Experiments 851101 and 851104: 0.01 M phosphate. (*B*) The ratio of blocked to unblocked single-channel current (i_B/i_0) as a function of [TEA^+] and membrane potential: (▲) +60 mV; (●) +30 mV; (■) −30 mV. The curves denote nonlinear least-squares fits to a single-site binding isotherms: $i_B/i_0(\max)\cdot K_B/(K_B + [TEA^+])$, where $i_B/i_0(\max)$ is the maximum value for i_B/i_0. At 60 mV, $K_B = 0.0114 \pm 0.0015$ M and $i_B/i_0(\max) = 1.00 \pm 0.05$. For the data at ±30 mV, $i_B/i_0(\max)$ was assigned a value of 1. At +30 mV, $K_B = 0.020 \pm 0.002$ M; at −30 mV, $K_B = 0.050 \pm 0.002$ M.

voltage independent, and that Ba^{++} does not bind with high affinity at a site deep within the channel. In contrast, the addition of Ba^{++} to only the extracellular solution produced what appears to be a weakly voltage-dependent current reduction (Fig. 11). While the shape of the *i-V* relation could suggest a bona fide

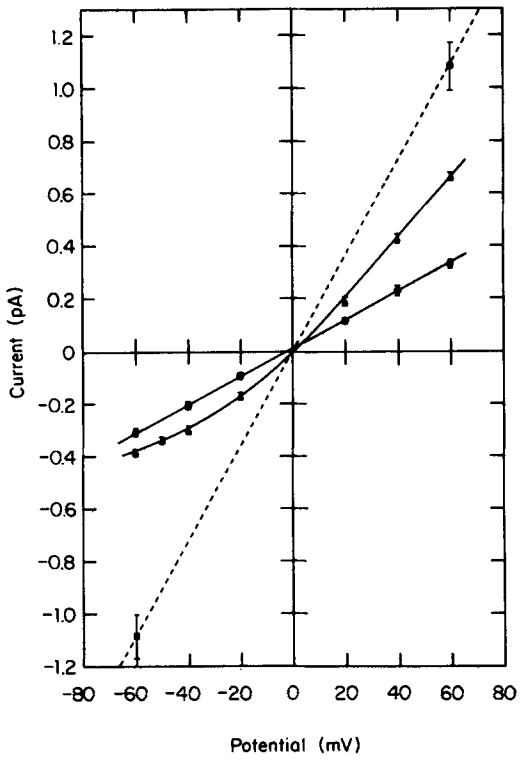

FIGURE 11. Effects of Ba^{++} on the single-channel current. (▲) *i-V* relation in symmetrical 0.02 M Na^{+} with 0.005 M Ba^{++} added to the extracellular solution. The curve through points has no theoretical significance. (●) *i-V* relation in symmetrical 0.02 M Na^{+} with 0.005 M Ba^{++} added to both solutions. The line through the points denotes a linear regression to the data. The conductance was 5.4 pS. The dashed line represents the average *i-V* relation in 0.02 M Na^{+} in the absence of Ba^{++}. Experiments 860130 and 860131: 0.005 M HEPES.

voltage-dependent block, the more likely explanation is that Ba^{++} screens, or binds to, negative charges at the channel entrance.

In symmetrical solutions of Na^{+} and Zn^{++}, the *i-V* relation is not linear (data not shown), and extracellular Zn^{++} caused a pronounced voltage-dependent current reduction consistent with Zn^{++} exerting its major effect through a voltage-dependent block (Fig. 12). Qualitatively similar results were observed by adding Ca^{++} to the extracellular solution (data not shown). The open-channel

current noise was not affected by the divalent cations (e.g., Fig. 12*A*). When we fitted Eq. 1 to the data, the estimates of $K_B(0)$ and δ for Zn^{++} were $9 \pm 7 \times 10^{-4}$ M (range, 3–16 $\times 10^{-4}$ M in three experiments) and 0.21 ± 0.03; for Ca^{++}, $K_B(0)$ and δ were $1.3 \pm 0.1 \times 10^{-3}$ M and 0.18 ± 0.03. The similar δ estimates suggest that these divalent cations bind and block at a common site.

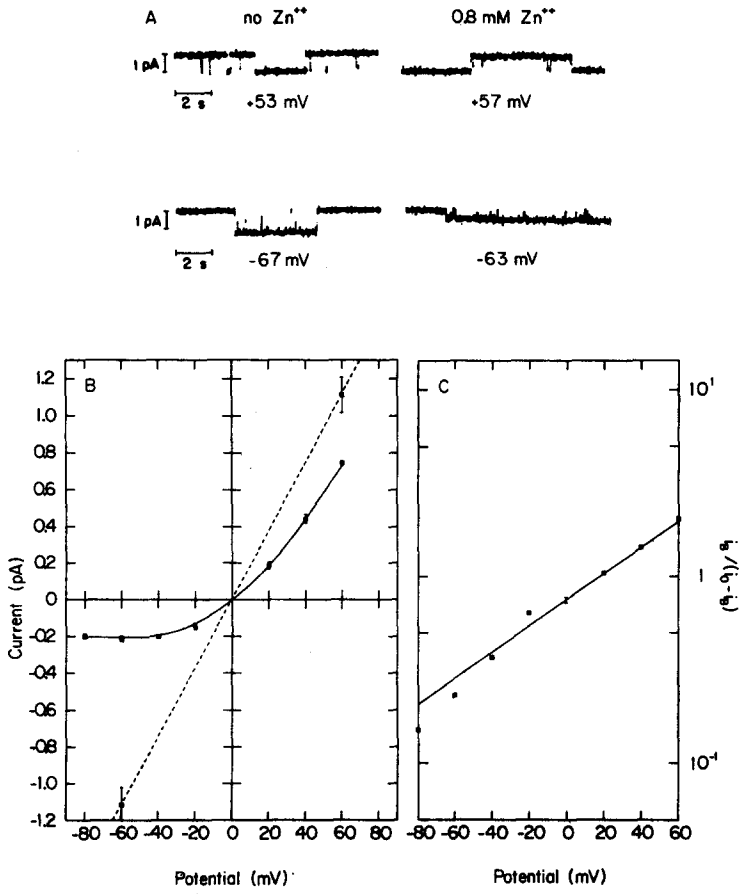

FIGURE 12. Effects of extracellular Zn^{++} on the single-channel current. (*A*) Current traces in symmetrical 0.02 M Na^+, before and after the addition of 0.0008 M Zn^{++} to the extracellular solution, illustrate the voltage dependence of the block. At positive potentials, channel openings are upward; at negative potentials, they are downward. Experiment 841120: 0.005 M HEPES. (*B*) *i-V* relation in the presence of 0.0008 M extracellular Zn^{++}. The solid curve has no theoretical significance. The dashed line represents the average *i-V* relation in 0.02 M Na^+ in the absence of Zn^{++}. Experiment 841025: 0.005 M HEPES. (*C*) Voltage dependence of the block by extracellular Zn^{++}. The data from *B* were plotted as $i_B/(i_0 - i_B)$ vs. ΔV. The line denotes a fit of Eq. 1 to the data: $K_B = 6.0 \pm 0.2 \times 10^{-4}$ M; $\delta = 0.21 \pm 0.01$.

DISCUSSION

BTX-modified sodium channels incorporated into planar lipid bilayer membranes are qualitatively similar to sodium channels in biological membranes. The ion selectivity, STX and TTX sensitivity, voltage-activation characteristics, and single-channel conductances are all comparable, as emphasized previously (Krueger et al., 1983; Moczydlowski et al., 1984). Some differences may exist between BTX-modified sodium channels in biological and planar bilayer membranes (see below). These differences do not throw into question the general identification of the bilayer-incorporated channels, but they do raise a question regarding their exact molecular identity: are the bilayer-incorporated channels representative of sodium channels in the synaptosome suspension (or the central nervous system of the dog), or does a subpopulation of sodium channels incorporate selectively? (Three distinct mRNA's for sodium channels have been found in the rat brain [Noda et al., 1986].) This is a general problem for studies based on very small ($\sim 10^{-24}$ mol) samples of a substance (see also Mazet et al., 1984). There is no readily available way to assess the severity of this problem in the bilayer and we will, in the absence of contrary evidence, proceed on the assumption that bilayer-incorporated BTX-modified sodium channels are fully intact and are representative of BTX-modified channels in situ.

In this study, some features of ion movement through open sodium channels have been inferred from measurements on the single-channel conductance as a function of the concentration of permeant and impermeant cations. These features are: a net negative charge at channel entrances that increases the conductance by increasing the local $[Na^+]$; at least two cation-binding sites in the permeation path; and an asymmetric permeation path. Before discussing these aspects of channel function, we will briefly discuss our results on channel incorporation and disappearance.

Channel Incorporation and Disappearance

Several features of sodium channel incorporation are consistent with the channels incorporating by fusion of outside-out vesicles with the bilayer: more than a single channel could incorporate simultaneously; the number of channels per incorporation event could be approximated by a Poisson distribution; and, when the bilayer was not broken, the channels incorporated with their extracellular surface facing the chamber into which the vesicles were added. The average number of sodium channels per incorporation is 1.5 (see Table I), but there are 20–100 STX receptors per synaptosome (the average surface area of a synaptosome is ~ 1 μm^2, and the surface density of STX receptors is $20–100/\mu m^2$ [Catterall, 1984]). If synaptosomes fused with the bilayer, a much larger number of channels per incorporation would be expected. The low number observed in this study may result from a preferential incorporation of the smaller vesicles that are present in synaptosomal preparations (e.g., Hajos, 1975, Fig. 2). (Note, however, that the number of incorporations with four or more channels is larger than predicted from the Poisson distribution.)

The Poisson frequency distribution of channels per incorporation suggests

that each sodium channel is an independent entity, i.e., that the channels are not organized together as oligomers. Additional support for channel independence is that single channels could be isolated after multichannel incorporations (Fig. 1). Since sodium channels can cluster in biological membranes (Almers et al., 1983; Beam et al., 1985), the absence of clustering in bilayers indicates that clustering may be mediated by something that is lost by the preparation of the synaptic membranes or by incorporation into the bilayer (e.g., cytoskeletal attachments).

The spontaneous channel disappearances could result from the dissociation of BTX from the channel, which should cause the reappearance of channel inactivation and a loss of the steady state activation. If these channel disappearances are caused exclusively by BTX dissociation, the average residence time for BTX is 250 min at 24°C. Given the difference in temperature, this estimate is comparable to the average residence times in neuroblastoma cells at 36°C, 40–80 min (Catterall, 1975).

Ion Selectivity

The ion selectivity of BTX-modified sodium channels is less than that of their unmodified counterparts (e.g., Khodorov, 1985). In myelinated nerve, estimates for P_K/P_{Na} for unmodified channels range from 0.086 for unmodified channels (Hille, 1972) to ~0.19 for BTX-modified channels (Mozhayeva et al., 1983*b*). (Khodorov and Revenko [1979] obtained a larger value for P_K/P_{Na}, 0.40, but this estimate may have been affected by changes in the intracellular ionic composition [see Andersen et al., 1986, for further discussion].) In neuroblastoma cells, P_K/P_{Na} increased from ~0.1 in unmodified channels to ~0.4 (Huang et al., 1982), while measurements of unidirectional cation fluxes through BTX-modified channels in cloned neuroblastoma cells gave P_K/P_{Na} estimates of 0.17 in a cell line with normally TTX-sensitive sodium channels (Huang et al., 1979).

Our estimate for P_K/P_{Na} in BTX-modified sodium channels (~0.16) agrees with the estimates for BTX-modified sodium channels in biological membranes. Similar permeability or conductance ratio estimates for BTX-modified sodium channels were also obtained by Tanaka et al. (1983) and Hartshorne et al. (1985) for channels purified from rat muscle or brain, and reconstituted into lipid vesicles or planar lipid bilayers. Other studies on BTX-modified sodium channels incorporated into planar bilayers reported P_K/P_{Na} to be ~0.07 for rat brain and muscle channels (Krueger et al., 1983; Moczydlowski et al., 1984).

In squid giant axon sodium channels, P_K/P_{Na} varies with the electrolyte composition in the intracellular fluid (Chandler and Meves, 1965; Cahalan and Begenisich, 1976). This composition dependence has been interpreted to reflect multiple ion occupancy in the channel (Begenisich and Cahalan, 1980*a*). In contrast, there is no evidence for interactions among permeant ions in BTX-modified sodium channels because P_K/P_{Na}, within experimental error, was invariant with respect to changes in the ionic composition of either the extracellular or the intracellular solutions. The absence of ion interactions is probably a consequence of the BTX modification, since many ions that block native sodium channels from the intracellular solution have much less affinity for BTX-modified

sodium channels (e.g., Khodorov, 1985). One or more cation-binding sites in the channel seem to be altered by BTX modification.

Conductance vs. [Na^+]

The determination of the g-[Na^+] relation was affected by the existence of several conductance states, which imposed a practical limit on how far we could decrease the [Na^+]. The situation may be similar to that for sarcoplasmic reticulum potassium channels, where problems precluded conductance determinations at salt concentrations <0.015 M (Cukierman et al., 1986). Undetected flickery activity at low salt may artifactually decrease the estimated single-channel currents and depress the g-[Na^+] relation at [Na^+] < 0.1 M, and our conductance estimates at 0.02 and 0.05 M Na^+ should be regarded as lower limits. The different conductance states described here have not been reported for other BTX-modified sodium channels. The reason for this difference is not clear, but dog brain sodium channels may differ from other sodium channels. We do not advocate this position, but note that pharmacological dissections provide evidence for (tissue-specific) sodium channel subtypes (Moczydlowski et al., 1986*a*).

Conductance (or current) vs. [Na^+] relations have been determined for sodium channels on frog node of Ranvier (Drouin and Neumcke, 1974; Hille, 1975*a*, *b*) and in squid giant axon (Begenisich and Cahalan, 1980*b*; Spires, 1985; Yamamoto et al., 1985). The experiments were done at a constant ionic strength, and the conductance vs. [Na^+] relations could be approximated as Langmuir isotherms:

$$G = G_{max} \cdot [Na^+]/(K_G + [Na^+]), \quad (2)$$

where G denotes the membrane's sodium conductance, G_{max} denotes the maximum sodium conductance, and K_G denotes the [Na^+] for half-maximal conductance. The estimates for K_G were >0.3 M in the frog node and 0.4–1 M in the squid axon.

The sodium conductance decreases as the extracellular (Hille, 1968; Woodhull, 1973; Mozhayova et al., 1982; Begenisich and Danko, 1983) or intracellular solution is acidified (Wanke et al., 1980). From the pH and voltage dependence of this H^+-induced block, it appears that the rate of Na^+ permeation through the channel is affected by at least two titratable groups, probably carboxyl groups, that are accessible from the extracellular solution. One group is in the permeation path (Woodhull, 1973; Mozhayeva et al., 1982; Begenisich and Danko, 1983); another is quite superficial at the extracellular entrance (Mozhayeva et al., 1982).

Unlike the experiments on native sodium channels, our determination of the g-[Na^+] relation for bilayer-incorporated sodium channels was done without a support electrolyte, i.e., at a varying ionic strength. Not surprisingly, the g-[Na^+] relation in Fig. 6*A* cannot be described by a Langmuir isotherm. Qualitatively, the deviations from the shape described by the simple saturating function (e.g., Eq. 2) could result from a net negative charge at one or both channel entrances, which would act to increase the local [Na^+] relative to the bulk phase concentration. The g-[Na^+] relation could also result from multiple ion occupancy (e.g., Urban and Hladky, 1979). While multiple Na^+ occupancy cannot be excluded, it is unlikely to be the dominant factor in determining the shape of the g-[Na^+]

relation, because the results of the reversal potential measurements suggest that there are no interactions among permeant anions. As a first approximation, we therefore analyze the data assuming that, at most, one Na^+ can occupy a BTX-modified sodium channel at any time.

A net negative charge at the channel entrance will give rise to a potential difference, V_e, between the bulk aqueous phase and the entrance region. V_e depends on the geometry and charge distribution of the entrance region as well as the ionic composition of the adjacent aqueous phase. In the absence of structural information, V_e was calculated using the Gouy-Chapman equation (e.g., Aveyard and Haydon, 1973):

$$V_e = (2 \cdot kT/e) \cdot \text{arcsinh}\{\sigma/(8 \cdot [Na^+] \cdot \epsilon_o \cdot \epsilon_r \cdot kT)\}^{0.5}, \quad (3)$$

where σ is an apparent charge density at the entrance, ϵ_o is the permittivity of free space, and ϵ_r is the relative dielectric constant of water (78.5 at 24°C [Weast, 1972, p. E-49]). (The presence of $HPO_4^=$ was ignored; this will not affect the estimates for V_e.) The relation between the local $[Na^+]$ at the entrance, $[Na^+]_e$, and the bulk $[Na^+]$ was approximated by a Boltzmann distribution:

$$[Na^+]_e = [Na^+] \cdot \exp(-V_e \cdot e/kT). \quad (4)$$

In symmetrical salt solutions, if the geometries and charge distributions combine to produce similar V_e's at the intracellular and extracellular entrances, the g-$[Na^+]$ relation can be described by:

$$g = g_{max} \cdot [Na^+]/\{[Na^+] + K_{Na} \cdot \exp(V_e \cdot e/kT)\}. \quad (5)$$

The g-$[Na^+]$ data are well described by Eqs. 3–5 when $g_{max} \simeq 45$ pS, $K_{Na} \simeq 1.5$ M, and $\sigma \simeq -0.38\ e \cdot nm^{-2}$ (see Fig. 6). The K_{Na} estimate is consistent with the K_G estimates based on sodium current measurements in the frog node of Ranvier and squid giant axon when $[Na^+]$ is varied at a constant ionic strength. (In this approximate model, g approaches a finite limit not only as $[Na^+] \to \infty$, but also as $[Na^+] \to 0$, because the local $[Na^+]$ at the channel entrances according to the predictions of the Gouy-Chapman theory of the diffuse double layer will approach a lower limit, $\sigma^2/(2 \cdot \epsilon_o \cdot \epsilon_r \cdot kT)$, as the bulk $[Na^+] \to 0$ [e.g., McLaughlin et al., 1971]. At 24°C, this limiting concentration is 1.08 M when $\sigma = -0.38\ e \cdot nm^2$, and the minimal conductance is ~19 pS. The practical determination of this limiting conductance, however, will be affected by the series resistance imposed by the aqueous phases.)

If negative charges at the entrances affect the channel's conductance, the conductance at low $[Na^+]$ should decrease when impermeant monovalent or divalent cations are added to the aqueous phases. When TEA^+ or Ba^{++} was added to both aqueous phases, the conductance decreased, which is consistent with screening of negative charges. Experiments where screening ions are added to only one side of the membrane are difficult to interpret. The electrostatic potential will change only at one entrance, thereby altering the permeant ion concentration at that entrance as well as the electrostatic field in the channel (e.g., Frankenhaeuser, 1960). The single-channel currents can thus change because of the different permeant ion concentrations at the entrances and

because of the change in electrical driving force. Both of these effects can account for the apparent voltage-dependent block observed when Ba^{++} is added to the extracellular side only (Fig. 11). To minimize any changes in electrostatic potential across the channel, the experiments to test for screening of fixed charges were therefore done using bilateral additions of impermeant monovalent or divalent cations. Evidence for the apparent success of this strategy is the linear *i-V* relation observed after the addition of Ba^{++} to both aqueous phases (Fig. 11). In this experiment, V_e can be calculated using the general Gouy-Chapman equation (e.g., Aveyard and Haydon, 1973, Eq. 2.29) and the predicted conductance is 6.6 pS, which should be compared with the measured value, 5.6 pS. For the TEA^+ additions, the predicted conductances were 13.5 pS in 0.05 M Na^+ plus 0.05 M TEA^+, and 6.6 pS in 0.02 M Na^+ plus 0.08 M TEA^+, which should be compared with the measured chord conductances at −80 mV, 13.5 and 8.2 pS, respectively (but see the next section). If a Langmuir isotherm is fitted to these conductances determined at a constant ionic strength, g_{max} = 38 pS, whereas K_g, the $[Na^+]$ for half-maximal conductance, is 0.08 M. At an ionic strength of 0.1 M, V_e = −65 mV when $\sigma = -0.38\ e\cdot nm^{-2}$, and the local $[Na^+]$ at the entrance will be ~13 times larger than the bulk $[Na^+]$. K_{Na} is thus estimated to be ~1 M.

The *g*-$[Na^+]$ relations for BTX-modified sodium channels from rat muscle and brain have been approximated by Langmuir isotherms (Moczydlowski et al., 1984; Worley et al., as reported in Coronado, 1986). Qualitatively, between 0.02 and 0.1 M Na^+, the single-channel conductances are fairly similar among the channels studied. The dashed line in Fig. 6*B* denotes a fit of a Langmuir isotherm to this restricted data set. Quantitatively, the estimates of K_{Na} and g_{max} for the rat channels differ from those for the dog channels because conductance values at $[Na^+] > 0.5$ M were included in our analysis and because different equations were fitted to the data. When we restricted the analysis to the data at $[Na^+] \leq 0.5$ M, a fit of Eqs. 3–5 to the subset gave the estimates $K_{Na} \simeq 0.48$ M, $\sigma \simeq -0.27\ e\cdot nm^{-2}$, and $g_{max} \simeq 35$ pS, $\chi^2 = 1.3$. A fit of a Langmuir isotherm to the subset gave the estimates g_{max} = 25 pS, K_g = 0.012 M, $\chi^2 = 7.8$. The two fits can be compared using the *F* test (Ellis and Dugglesby, 1978). In the present case, *F* is 14.7 and the probability of exceeding *F* is <0.1. It is unlikely that our conclusion, that there are functionally significant negative charges at the channel entrances, should be ascribed to some nonspecific effect of high $[Na^+]$. (Additional support for functionally important negative charges at the extracellular channel entrance is that H^+ blocks the sodium conductance in the frog node of Ranvier and squid giant axon [*vide supra*], and that carboxylate group–specific reagents react with the extracellular surface of sodium channels to decrease the single-channel conductance [Sigworth and Spalding, 1980; Worley et al., 1986; Chabala et al., 1986]. The interpretation of the covalent modification experiments is ambiguous, however, because it cannot be excluded that [at least some of] the single-channel conductance decrease could result from conformational changes consequent to modifications at other parts of the channel.)

Charges on the host lipid bilayer have no measurable effect on the single-channel conductances in 0.1 and 0.5 M Na^+, which suggests that the entrances

are >2 nm from the bilayer/solution interfaces. This structural interpretation is uncertain, however, because small contributions of the lipid bilayer surface charge to V_e may be obscured by charges on the sodium channel.

Screening and Block

When added to the extracellular solution, TEA^+ decreases single-channel currents, which is consistent with a screening of fixed charges at the extracellular channel entrance. When added to the intracellular solution, TEA^+ induces a voltage-dependent block. The increased current noise (Figs. 9*A* and 10*A*) and the shape of time-averaged single-channel *i-V* relations (e.g., Yellen, 1984) suggest that TEA^+ enters the channel by the intracellular entrance, and binds some distance into the channel, thereby blocking ion movement.

The dual effects of intracellular TEA^+, the reduction of the electrostatic potential at the entrance, and the voltage-dependent block are not independent of one another. Changes in the electrostatic potential, V_e, will again alter the degree of channel block by altering the local concentrations of the blocking and permeant ions. Importantly, since V_e will vary as a function of the bulk electrolyte composition, the dose-response curve for the block may not necessarily follow a simple inhibition curve, $i_B = i_0 \cdot K_B/(K_B + [B])$ (e.g., Edsall and Wyman, 1958; McLaughlin, 1977). If there are competive interactions between the blocking and permeant ions and if V_e varies as a function of the blocking ion concentration, the shape of the dose-response curve will depend on whether the blocking ion is monovalent or divalent (Green and Andersen, 1986, Fig. 2). The dose-response curve may appear to be a simple inhibition curve if the relevant ions have the same valence, because the relative change in the local concentrations will be the same for these ions. Because Na^+ may compete with TEA^+ at the intracellular channel entrance, it is not surprising that the dose-response curve for TEA^+-induced block could be described by a Langmuir isotherm (Fig. 10*B*) (see also Green and Andersen, 1986; Green et al., 1987).

Part of the conductance decreases observed at −80 mV with bilateral additions of TEA^+ may result from TEA^+-induced block at the intracellular entrance. Corrections for this block depend on the underlying model, especially the assumption that there are no interactions between Na^+ and TEA^+ in the channel. This assumption may be questioned because increasing the extracellular [Na^+] relieves the block by several intracellular channel blockers (Shapiro, 1977; Cahalan and Almers, 1979).

The voltage dependence of the channel block induced by intracellular TEA^+ was analyzed using the Woodhull (1973) model. Estimates for δ were ~0.5 for [TEA^+] varying between 0.002 and 0.04 M (Fig. 9*C*). This estimate is comparable to the δ values determined for other compounds (tetramethylammonium, methylguanidinium, and butylguanidinium) that block bilayer-incorporated BTX-modified sodium channels from the intracellular solution (Moczydlowski et al., 1986*b*), which indicates that these compounds all bind at a common site. (The δ estimate may not, however, be a good indicator of the electrical distance from the intracellular solution to the binding site. Comparisons with more detailed models suggest that the Woodhull model underestimates the actual voltage dependence [Andersen, O. S., manuscript in preparation].)

In addition to their screening action, extracellular Zn^{++} and Ca^{++} also block sodium channels. The voltage dependence of the block was again interpreted using the Woodhull model. The estimate for δ (~0.2) is similar to that obtained for Ca^{++} in native and BTX-modified channels (Woodhull, 1973; Mozhayeva et al., 1983*a*; Moczydlowski et al., 1986*a*; Worley et al., 1986). The Ca^{++}-induced block is reduced when the $[Na^+]$ is increased and when Na^+ is replaced by permeant cations that are presumed to have higher affinities for the channel, i.e., ions that have smaller K_G values (Yamamoto et al., 1985). This apparent competition suggests that the site of block is within the permeation path.

Characteristics of the Ion Permeation Path

The voltage-dependent channel block induced by TEA^+, Ca^{++}, and Zn^{++} suggests that there is a minimum of two cation-binding sites in the channel and that the sites are not symmetrical with respect to the electric potential profile. One site, accessible from the extracellular solution, has an electrical distance from that solution of ~0.2. The other site, accessible from the intracellular solution, has an electrical distance from that solution of at least 0.5. Different blocking cations interact differently with these sites. Ca^{++} and Zn^{++} block at the site accessible to the extracellular solution, but TEA^+ and Ba^{++} do not appear to bind to this site. TEA^+ binds to the site accessible to the intracellular solution, but Ba^{++} and Zn^{++} do not appear to bind to this site. This asymmetry of block suggests that there is a significant barrier for ion movement at an electrical distance between 0.2 and 0.5 from the extracellular solution. Additionally, the differential effects of intracellular and extracellular K^+ on the *i-V* relations (Fig. 8) show that intracellular K^+ blocks Na^+ movement through the channel. Since K^+ is permeant, the block probably results from K^+ binding at a site within the permeation path. Because of the asymmetry of the block, the major barrier (i.e., the selectivity filter) for K^+ must lie between this site and the extracellular solution. The selectivity filter for K^+ may be the barrier that was deduced from the TEA^+ and Zn^{++} blocking experiments.

Since Zn^{++} and Ca^{++} are smaller than TEA^+, steric restrictions cannot explain the asymmetry in the Ca^{++}-induced (Moczydlowski et al., 1986*a*) or the Zn^{++}-induced block. Equilibrium ion binding to the extracellular and intracellular binding sites must be different. Using the terminology of Eisenman (e.g., Eisenman and Horn, 1983), the extracellular binding site seems to be a high-field-strength site, while the intracellular site seems to be a (hydrophobic) low-field-strength site. Whether this conclusion holds for native as well as BTX-modified channels remains to be seen (see Khodorov, 1985). Similar reasoning cannot be used to interpret the asymmetry of the TEA^+-induced block, because we cannot distinguish between steric restrictions to TEA^+ entry and low binding affinity to the extracellular site.

Negative charges at the channel entrance(s) may be important for the primary function of open sodium channels: to facilitate rapid and selective movement of Na^+ across cell membranes. To accomplish this function, the channel must act as a sink for ion entry and yet allow the ions to leave at a rapid rate. On the basis of our measurements, the channel meets both criteria. The dissociation rate constant for Na^+ at 0 mV is high, $\sim 3 \times 10^7\ s^{-1}$. In addition, the intrinsic Na^+

affinity of the channel appears to be weak, at least for the dog brain sodium channel, with a K_{Na} of 1–1.5 M. Note, however, that if no mechanism exists to increase the [Na^+] at the entrances, the single-channel conductance at physiological ionic conditions would be ~1/10 of the maximal conductance. A net negative charge at the entrances will increase the channel's conductance by increasing the local [Na^+] and the effective rate constant for ion entry. Such charges may serve to overcome any diffusion limitations for ion access to the channel's selectivity filter (Andersen, 1983*b*). A net negative charge at the extracellular entrance will have the additional advantage that the single-channel currents should become comparatively insensitive to the Na^+ depletion that may occur during an action potential (e.g., Neumcke and Stämpfli, 1983). Negative charges at the channel entrances may have evolved to increase the net charge movement per channel during an action potential.

We thank J. W. Daly, National Institutes of Health, for the generous gifts of BTX, and P. Siekevitz's laboratory (The Rockefeller University) for making the synaptosomes available to us. We also thank J.-L. Mazet for encouragement during the initial stages of this work, R. J. French, B. K. Krueger, and J. F. Worley for freely sharing their expertise with us, L. D. Chabala and B. W. Urban for helpful discussions, and D. B. Cherbavaz for the artwork.

This work was supported by grant GM-21342 and training grant AM-07152 from the National Institutes of Health, and by the Departmental Associates Program at Cornell University Medical College.

Original version received 15 July 1986 and accepted version received 16 February 1987.

REFERENCES

Almers, W., P. R. Stanfield, and W. Stühmer. 1983. Lateral distribution of sodium and potassium channels in frog skeletal muscle: measurement with a patch-clamp technique. *Journal of Physiology.* 336:261–284.

Andersen, O. S. 1983*a*. Ion movement through gramicidin A channels. Single-channel measurements at very high potentials. *Biophysical Journal.* 41:119–133.

Andersen, O. S. 1983*b*. Ion movement through gramicidin A channels. Studies on the diffusion-controlled association step. *Biophysical Journal.* 41:147–165.

Andersen, O. S., W. N. Green, and B. W. Urban. 1986. Ion conduction through sodium channels in planar lipid bilayers. *In* Ion Channel Reconstitution. C. Miller, editor. Plenum Publishing Corp., New York. 385–404.

Andersen, O. S., and R. U. Muller. 1982. Monazomycin-induced single channels. I. Characteristics of the elementary conductance events. *Journal of General Physiology.* 80:403–426.

Aveyard, R., and D. A. Haydon. 1973. An Introduction to the Principles of Surface Chemistry. Cambridge University Press, London. 232 pp.

Barchi, R. L. 1983. Protein components of the purified sodium channel from rat skeletal muscle sarcolemma. *Journal of Neurochemistry.* 40:1377–1385.

Beam, K. G., J. H. Caldwell, and D. T. Campbell. 1985. Na channels in skeletal muscle concentrated near the neuromuscular junction. *Nature.* 313:588–590.

Begenisich, T. B., and M. D. Cahalan. 1980*a*. Sodium channel permeation in squid axons. I. Reversal potential experiments. *Journal of Physiology.* 307:217–242.

Begenisich, T. B., and M. D. Cahalan. 1980*b*. Sodium channel permeation in squid axons. II. Non-independence and current-voltage relations. *Journal of Physiology.* 307:243–257.

Begenisich, T. B., and M. Danko. 1983. Hydrogen ion block of the sodium pore in squid giant axons. *Journal of General Physiology.* 82:599–618.

Bevington, P. R. 1969. Data Reduction and Error Analysis for the Physical Sciences. McGraw-Hill, New York. 336 pp.

Cahalan, M. D., and W. Almers. 1979. Interactions between quaternary lidocaine, the sodium channel gates, and tetrodotoxin. *Biophysical Journal.* 27:39–56.

Cahalan, M. D., and T. B. Begenisich. 1976. Sodium channel selectivity. Dependence on internal permeant ion concentration. *Journal of General Physiology.* 68:111–125.

Catterall, W. A. 1975. Activation of the action potential Na^+ ionophores of cultured neuroblastoma cells by veratridine and batrachotoxin. *Journal of Biological Chemistry.* 250:4053–4059.

Catterall, W. A. 1984. The molecular basis of neuronal excitability. *Science.* 223:653–661.

Chabala, L. D., W. N. Green, O. S. Andersen, and C. L. Borders, Jr. 1986. Covalent modification of external carboxyl groups of batrachotoxin-modified canine forebrain sodium channels. *Biophysical Journal.* 49:49*a*. (Abstr.)

Chandler, W. K., A. L. Hodgkin, and H. Meves. 1965. The effect of changing the internal solution on sodium inactivation and related phenomena in giant axons. *Journal of Physiology.* 180:821–836.

Chandler, W. K., and H. Meves. 1965. Voltage clamp experiments on internally perfused giant axons. *Journal of Physiology.* 180:788–820.

Cohen, F. S. 1986. Fusion of liposomes to planar bilayers. *In* Ion Channel Reconstitution. C. Miller, editor. Plenum Publishing Corp., New York. 131–139.

Cohen, R. S., F. Blomberg, K. Berzins, and P. Siekevitz. 1977. The structure of postsynaptic densities isolated from dog cerebral cortex. I. Overall morphology and protein composition. *Journal of Cell Biology.* 74:181–203.

Coronado, R. 1986. Recent advances in planar phospholipid bilayer techniques for monitoring ion channels. *Annual Review of Biophysics and Biophysical Chemistry.* 15:259–277.

Cukierman, S., G. Yellen, and C. Miller. 1986. The K^+ channel of sarcoplasmic reticulum. A new look at Cs^+ block. *Biophysical Journal.* 48:477–484.

Daly, J. W., G. B. Brown, M. Mensah-Dwumah, and C. W. Myers. 1978. Classification of skin alkaloids from neotropical poison-dark frogs (*Dendrobatidae*). *Toxicon.* 16:163–188.

Danko, M., C. Smith-Maxwell, L. McKinney, and T. Begenisich. 1986. Block of sodium channels by internal mono- and divalent guanidinium analogues. Modulation by sodium ion concentration. *Biophysical Journal.* 49:509–520.

Drouin, H., and B. Neumcke. 1974. Specific and unspecific charges at the sodium channels of the nerve membrane. *Pflügers Archiv.* 351:207–229.

Edsall, J. T., and J. Wyman. 1958. Biophysical Chemistry, Vol. I. Academic Press, Inc., New York. 699 pp.

Eisenman, G., and R. Horn. 1983. Ionic selectivity revisited: the role of kinetic and equilibrium processes in ion permeation through channels. *Journal of Membrane Biology.* 76:197–225.

Ellis, K. J., and R. G. Duggleby. 1978. What happens when data are fitted to the wrong equation. *Biophysical Journal.* 171:513–517.

Frankenhaeuser, B. 1960. Sodium permeability in toad nerve and squid axon. *Journal of Physiology.* 152:159–166.

Frankenhaeuser, B., and A. L. Hodgkin. 1957. The action of calcium on the electrical properties of squid axons. *Journal of Physiology.* 137:218–244.

Green, W. N., and O. S. Andersen. 1986. Surface charges near the guanidinium neurotoxin binding site. *Annals of the New York Academy of Sciences.* 479:306–312.

Green, W. N., L. B. Weiss, and O. S. Andersen. 1986. The tetrodotoxin and saxitoxin binding site of voltage-dependent sodium channels is negatively charged and distant from the permeant pathway. *Biophysical Journal.* 49:40*a*. (Abstr.)

Green, W. N., L. B. Weiss, and O. S. Andersen. 1987. Batrachotoxin-modified sodium channels in planar lipid bilayers. Characterization of saxitoxin- and tetrodotoxin-induced channel closures. *Journal of General Physiology.* 89:873–903.

Hajos, F. 1975. An improved method for the preparation of synaptosomal fractions in high purity. *Brain Research.* 93:485–489.

Hartshorne, R. P., B. U. Keller, J. A. Talvenheimo, W. A. Catterall, and M. Montal. 1985. Functional reconstitution of the purified brain sodium channel into planar lipid bilayers. *Proceedings of the National Academy of Sciences.* 82:240–244.

Hille, B. 1968. Charges and potentials at the nerve surface. Divalent ions and pH. *Journal of General Physiology.* 51:221–236.

Hille, B. 1972. The permeability of the sodium channel to metal cations in myelinated nerve. *Journal of General Physiology.* 59:637–658.

Hille, B. 1975*a*. Ionic selectivity of Na and K channels of nerve membranes. *In* Membranes: a Series of Advances. Dynamic Properties of Lipid Bilayers and Biological Membranes. G. Eisenman, editor. Marcel Dekker, New York. 3:255–323.

Hille, B. 1975*b*. Ionic selectivity, saturation, and block in sodium channels. A four-barrier model. *Journal of General Physiology.* 66:535–560.

Hille, B., A. M. Woodhull, and B. I. Shapiro. 1975. Negative surface charge near sodium channels of nerve: divalent ions, monovalent ions, and pH. *Philosophical Transactions of the Royal Society of London, Series B.* 270:301–318.

Hodgkin, A. L., and B. Katz. 1949. The effect of sodium ions on the electrical activity of the giant axon of the squid. *Journal of Physiology.* 108:37–77.

Huang, L. M., W. A. Catterall, and G. Ehrenstein. 1979. Comparison of ionic selectivity of batrachotoxin-activated channels with different tetrodotoxin dissociation constants. *Journal of General Physiology.* 73:839–854.

Huang, L. M., N. Moran, and G. Ehrenstein. 1982. Batrachotoxin modifies the gating kinetics of sodium channels in internally perfused neuroblastoma cells. *Proceedings of the National Academy of Sciences.* 79:2082–2085.

Khodorov, B. I. 1985. Batrachotoxin as a tool to study voltage-sensitive sodium channels of excitable membranes. *Progress in Biophysics and Molecular Biology.* 45:57–148.

Khodorov, B. I., and S. V. Revenko. 1979. Further analysis of the mechanisms of action of batrachotoxin on the membrane of myelinated nerve. *Neuroscience.* 4:1313–1340.

Kirsch, G. E., J. Z. Zeh, J. M. Farley, and T. Narahashi. 1980. Interactions of *n*-alkylguanidines with the sodium channels of squid axon membrane. *Journal of General Physiology.* 76:315–335.

Krueger, B. K., J. F. Worley, and R. J. French. 1983. Single sodium channels from rat brain incorporated into planar lipid bilayer membranes. *Nature.* 303:172–175.

Mazet, J.-L., O. S. Andersen, and R. E. Koeppe II. 1984. Single-channel studies on linear gramicidins with altered amino acid sequences. A comparison of phenylalanine, tryptophane, and tyrosine substitutions at position 1 and 11. *Biophysical Journal.* 45:263–276.

McLaughlin, S. 1977. Electrostatic potentials at membrane-solution interfaces. *Current Topics in Membranes and Transport.* 9:71–144.

McLaughlin, S. G. A., G. Szabo, and G. Eisenman. 1971. Divalent ions and surface potential of charged phospholipid membranes. *Journal of General Physiology.* 58:667–687.

Messner, D. J., and W. A. Catterall. 1985. The sodium channel from rat brain. Separation and characterization of subunits. *Journal of Biological Chemistry.* 260:10597–10604.

Miller, C., and E. Racker. 1976. Ca^{++}-induced fusion of fragmented sarcoplasmic reticulum with artificial bilayers. *Journal of Membrane Biology.* 30:283–300.

Miller, J. A., W. S. Agnew, and S. R. Levinson. 1983. Principal glycopeptide of the tetrodotoxin/saxitoxoin binding protein from *Electrophorus electricus*: isolation and partial chemical and physical characterization. *Biochemistry.* 22:462–470.

Moczydlowski, E., S. S. Garber, and C. Miller. 1984. Batrachotoxin-activated Na^+ channels in planar lipid bilayers. Competition of tetrodotoxin block by Na^+. *Journal of General Physiology.* 84:665–686.

Moczydlowski, E., A. Uehara, X. Guo, and J. Heiny. 1986*a*. Isochannels and blocking modes of voltage-dependent sodium channels. *Annals of the New York Academy of Sciences.* 479:269–292.

Moczydlowski, E., A. Uehara, and S. Hall. 1986*b*. Blocking pharmacology of batrachotoxin-activated Na-channels from rat skeletal muscle. *In* Ion Channel Reconstitution. C. Miller, editor. Plenum Publishing Corp., New York. 405–428.

Mozhayeva, G. N., A. P. Naumov, and B. I. Khodorov. 1983*a*. Ionic current through batrachotoxin-modified sodium channels of the Ranvier node membrane at high positive and negative potentials. *Neirofiziologiya.* 15:495–503.

Mozhayeva, G. N., A. P. Naumov, and B. I. Khodorov. 1983*b*. Selectivity and sensitivity to hydrogen ion blocking of batrachotoxin-modified sodium channels in nerve fiber membrane. *Neirofiziologiya.* 15:571–579.

Mozhayeva, G. N., A. P. Naumov, and Y. A. Negulyaev. 1982. Interaction of H^+ ions with acid groups in normal sodium channels. *General Physiology and Biophysics.* 1:5–19.

Nagy, K., T. Kiss, and D. Hof. 1983. Single Na channels in mouse neuroblastoma cell membrane. Indications for two open states. *Pflügers Archiv.* 399:302–308.

Neumcke, B., and R. Stämpfli. 1983. Alteration of the conductance of Na^+ channels in the nodal membrane of frog nerve by holding potential and tetrodotoxin. *Biochimica et Biophysica Acta.* 727:177–184.

Noda, M., T. Ikeda, T., Kayano, H. Suzuki, H. Takeshima, M. Kurasaki, H. Takahashi, and S. Numa. 1986. Existence of distinct sodium channel messenger RNAs in rat brain. *Nature.* 320:188–192.

Noda, M., S. Simizu, T. Tanabe, T. Takai, T. Kayano, T. Ikeda, H. Takahashi, H. Nakayama, Y. Kanaoka, N. Minamino, K. Kangawa, H. Matsuo, M. Raftery, T. Hirose, S. Inayama, H. Hayashida, T. Miyata, and S. Numa. 1984. Primary structure of *Electrophorus electricus* sodium channel deduced from cDNA sequence. *Nature.* 312:121–127.

Plettig, V. 1930. Über die Diffusionspotentiale. *Annalen der Physik.* 5:735–761.

Rojas, E., and B. Rudy. 1976. Destruction of the sodium conductance inactivation by a specific protease in perfused nerve fibers from *Loligo*. *Journal of Physiology.* 262:501–531.

Salling, N., and O. Siggaard-Andersen. 1971. Liquid-junction potentials between plasma or erythrolysate and KCl solutions. *Scandinavian Journal of Clinical and Laboratory Investigations.* 28:33–40.

Shapiro, B. I. 1977. Effects of strychnine on the sodium conductance of the frog node of Ranvier. *Journal of General Physiology.* 69: 915–926.

Sigworth, F. J., and B. C. Spalding. 1980. Chemical modification reduces the conductance of sodium channels in nerve. *Nature.* 283:293–295.

Spires, S. 1985. Sodium channel saturation and alteration of current kinetics by several permeant ions. *Biophysical Journal.* 47:437*a*. (Abstr.)

Strichartz, G. R. 1973. The inhibition of sodium currents in myelinated nerve by quaternary derivatives of lidocaine. *Journal of Physiology.* 62:37–57.

Stühmer, W., and W. Almers. 1982. Photobleaching through glass micropipettes: sodium channels without lateral mobility in the sarcolemma of frog skeletal muscle. *Proceedings of the National Academy of Sciences.* 79:946–950.

Szabo, G., G. Eisenman, and S. Ciani. 1969. The effects of macrotetralide actin on the electrical properties of phospholipid bilayer membranes. *Journal of Membrane Biology.* 1:346–382.

Tanaka, J. C., J. F. Eccleston, and R. L. Barchi. 1983. Cation selectivity characteristics of the reconstituted voltage-dependent sodium channel purified from rat skeletal muscle sarcolemma. *Journal of Biological Chemistry.* 258:7519–7526.

Urban, B. W., and S. B. Hladky. 1979. Ion transport in the simplest single file pore. *Biochimica et Biophysica Acta.* 554:410–429.

Wanke, E., E. Carbone, and P. L. Testa. 1980. The sodium channel and intracellular H^+ blockage in squid axons. *Nature.* 287:62–63.

Weast, R. C. 1972. Handbook of Chemistry and Physics. The Chemical Rubber Co., Cleveland, OH.

Weiss, L. B., W. N. Green, and O. S. Anderson. 1984. Single channel studies on the gating of batrachotoxin (BTX)-modified sodium channels in lipid bilayers. *Biophysical Journal.* 45:67*a*. (Abstr.)

Woodhull, A. 1973. Ionic blockage of sodium channels in nerve. *Journal of General Physiology.* 84:361–377.

Worley, J. F., R. J. French, and B. K. Krueger. 1986. Trimethyloxonium modification of single batrachotoxin-activated sodium channels in planar bilayers. Changes in unit conductance and in block by saxitoxin and calcium. *Journal of General Physiology.* 87:327–349.

Yamamoto, D., J. Z. Yeh, and T. Narahashi. 1985. Interactions of permeant cations with sodium channels of squid axon membranes. *Biophysical Journal.* 48:361–368.

Yellen, G. 1984. Ion permeation and blockade in Ca^{++}-activated K^+ channels of bovine chromaffin cells. *Journal of General Physiology.* 82:157–186.